(3)

Semiannual Technical Report

Pseudomorphic Semiconducting Heterostructures from Combinations of AlN, GaN and Selected SiC Polytypes: Theoretical Advancement and its Coordination with Experimental Studies of Nucleation, Growth, Characterization and Device Development

Supported under Grant #N00014-90-J-1427
Office of the Chief of Naval Research
Report for the period 1/1/94–6/30/94

R. F. Davis, S. Kern, K. Linthicum, S. Roberson, S. Tanaka and V. Torres
Materials Science and Engineering Department
North Carolina State University
Campus Box 7907
Raleigh, NC 27695-7907

June, 1994

Semiannual Technical Report

Pseudomorphic Semiconducting Heterostructures from Combinations of AlN, GaN and Selected SiC Polytypes: Theoretical Advancement and its Coordination with Experimental Studies of Nucleation, Growth, Characterization and Device Development

Supported under Grant #N00014-90-J-1427
Office of the Chief of Naval Research
Report for the period 1/1/94–6/30/94

R. F. Davis, S. Kern, K. Linthicum, S. Roberson, S. Tanaka and V. Torres
Materials Science and Engineering Department
North Carolina State University
Campus Box 7907
Raleigh, NC 27695-7907

June, 1994

REPORT DOCUMENTATION PAGE

Form Approved
OMB No. 0704-0188

1. AGENCY USE ONLY *(Leave blank)*	2. REPORT DATE	3. REPORT TYPE AND DATES COVERED
	June, 1994	Semiannual Technical 1/1/94–6/30/94

4. TITLE AND SUBTITLE

Pseudomorphic Semiconducting Heterostructures from Combinations of AlN, GaN and Selected SiC Polytypes: Theoretical Advancement and its Coordination with Experimental Studies of Nucleation, Growth, Characterization and Device Development

5. FUNDING NUMBERS

414s007---01
1114SS
N00179
N66005
4B855

6. AUTHOR(S)

Robert F. Davis

7. PERFORMING ORGANIZATION NAME(S) AND ADDRESS(ES)

North Carolina State University
Hillsborough Street
Raleigh, NC 27695

8. PERFORMING ORGANIZATION REPORT NUMBER

N00014-90-J-1427

9. SPONSORING/MONITORING AGENCY NAMES(S) AND ADDRESS(ES)

Sponsoring: ONR, Code 314, 800 N. Quincy, Arlington, VA 22217-5660
Monitoring: Office of Naval Research Resider
The Ohio State University Research Center
1960 Kenny Road
Columbus, OH 43210-1063

10. SPONSORING/MONITORING AGENCY REPORT NUMBER

11. SUPPLEMENTARY NOTES

12a. DISTRIBUTION/AVAILABILITY STATEMENT

Approved for Public Release; Distribution Unlimited

12b. DISTRIBUTION CODE

13. ABSTRACT *(Maximum 200 words)*

AlN films with essentially atomically flat surfaces, indicative of two-dimensional growth have been deposited on on-axis 6H-SiC(0001) surfaces at 1050°C via plasma-assisted gas source MBE. Island features, the coalescence of which caused defects and influenced film quality, were observed on the vicinal surface. SiC/AlN pseudomorphic multilayers with abrupt interfaces and $(AlN)_x(SiC)_{1-x}$ solid solutions have been deposited using a similar technique and substrate. The use of on-axis substrates resulted in superior structures. High AlN solid solutions have been achieved; however, they were polycrystalline. Chemical interdiffusion between 6-H SiC wafers and deposited single crystal AlN thick films between 1800 and 1950°C was not observed via parallel electron energy loss microscopy and Auger depth profiles to within 15Å of the interface. Pseudomorphic GaN/AlGaN double heterostructures with abrupt interfaces have also been produced using GSMBE. The purpose is for UV light emitting diodes. A supersonic jet deposition system has been designed and commissioned for the growth of III-V nitride films.

14. SUBJECT TERMS

silicon carbide, aluminum nitride, gallium nitride, two dimensional growth, pseudomorphic heterostructures, molecular beam epitaxy, chemical interdiffusion, light emitting diodes, supersonic jet

15. NUMBER OF PAGES

32

16. PRICE CODE

17. SECURITY CLASSIFICATION OF REPORT	18. SECURITY CLASSIFICATION OF THIS PAGE	19. SECURITY CLASSIFICATION OF ABSTRACT	20. LIMITATION OF ABSTRACT
UNCLAS	UNCLAS	UNCLAS	SAR

Table of Contents

I. Introduction

The advent of techniques for growing semiconductor multilayer structures with layer thicknesses approaching atomic dimensions has provided new systems for both basic physics studies and device applications. Most of the research involving these structures has been restricted to materials with lattice constants that are equal within $\simeq 0.1\%$. However it is now recognized that interesting and useful pseudomorphic structures can also be grown from a much larger set of materials that have lattice-constant mismatches in the percent range. Moreover, advances in computer hardware and software as well as the development of theoretical structural and molecular models applicable for strained layer nucleation, growth and property prediction have occurred to the extent that the field is poised to expand rapidly. It is within this context that the research described in this report is being conducted. The materials systems of concern include combinations of the direct bandgap materials of AlN and GaN and selected, indirect bandgap SiC polytypes.

The extremes in thermal, mechanical, chemical and electronic properties of SiC allow the types and numbers of current and conceivable applications of this material to be substantial. However, a principal driving force for the current resurgence of interest in this material, as well as AlN and GaN, is their potential as hosts for high power, high temperature microelectronic and optoelectronic devices for use in extreme environments. The availability of thin film heterostructural combinations of these materials will substantially broaden the applications potential for these materials. The pseudomorphic structures produced from these materials will be unique because of their chemistry, their wide bandgaps, the availability of indirect/direct bandgap combinations, their occurrence in cubic and hexagonal forms and the ability to tailor the lattice parameters and therefore the amount of strain and the physical properties via solid solutions composed of the three components.

The research described in the following sections is concerned with (1) the effect of using vicinal versus on-axis 6-H-SiC(0001) substrates on the growth mode and on the surface and internal microstructural character of deposited AlN films, (2) the growth of AlN-SiC pseudomorphic heterostructures and $(AlN)_x(SiC)_{1-x}$ solid solutions by plasma-assisted gas-source molecular beam epitaxy, (3) the chemical interdiffusion between SiC and AlN, (4) the research thus far conducted in the development of an ultra-violet LED and (5) the development and commissioning of supersonic jet equipment for the growth of GaN films. These sections detail the procedures, results, discussions of these results, conclusions and plans for future research. Each subsection is self-contained with its own figures, tables, and references.

II. Initial Stage of Aluminum Nitride Film Growth on 6H-Silicon Carbide by Plasma-assisted, Gas-source Molecular Beam Epitaxy

A. Introduction

AlN has attractive characteristics such as a direct wide band gap of 6.28eV at 300K [1], high melting point of over 2275K [2], and a thermal conductivity of 3.2W/cmK [3]. Thus it is a candidate material for high power and high temperature microelectronic and optoelectronic applications. The multilayer heterostructures of GaN/AlN [4] and SiC/AlN [5] have also been considered interesting materials for the above mentioned applications. Recently, in addition to its device applications, AlN has been recognized the usefulness of this material as a buffer layer for the growth of GaN and InN on SiC and Sapphire substrates because of its intermediate lattice constant [6, 7, 8], e.g. the lattice constants of the *a*-axis of these materials are 3.189Å (2H-GaN), 3.112Å (2H-AlN) and 3.08Å (6H-SiC), and thermal expansion coefficient [6, 7]. It is of great importance to obtain very smooth and defect free AlN films in order to grow high-quality films subsequently. For the growth of multilayered structures such as GaN/AlN/SiC [8] and SiC/AlN/SiC [5], the smoothness of each layer would be especially desired. Smoothness in general is determined by growth modes, i.e. two-dimensional versus three dimensional growth. To obtain an atomically smooth surface, it should be necessary to grow films with a two-dimensional growth mode or step flow growth. In this study, the initial stages of AlN film growth on 6H-SiC substrates were investigated by cross-sectional HRTEM observation in terms of growth mode and defects at the interfaces. The effect of the vicinal surface of the substrate on AlN film growth is especially studied.

B. Experimental Procedure

AlN films were grown on Si faces of 6H-SiC (0001) substrates. The substrates used in this study were either on-axis or vicinal (3-4° off from (0001) toward <11$\bar{2}$0>) provided by Cree Research Inc. [9] All films were grown by plasma-assisted gas source molecular beam epitaxy under the same conditions. Solid Al (99.999% pure) was evaporated from a standard effusion cell. Nitrogen gas (99.9995% pure) was decomposed by an electron cyclotron resonance (ECR) plasma in the vicinity of the substrate. The detailed description of the deposition technique can be found in Ref.[10]. The as-received substrate was dipped in 10% HF solution for 5 min. to remove the surface protective silicon oxide layer (typically ~750Å in thickness), immediately followed by loading into MBE system. The substrate was annealed at 1050°C in an ultra high vacuum environmental (~1×10^{-9} torr) for 5 min. prior to the deposition in order to remove residual hydrocarbons and silicon oxide. The typical growth conditions are shown in Table I. In order to observe the initial stages of growth, the thickness of the films was controlled by varying the growth time. After growing the film, the sample was cut and glued

face to face to make a cross-sectional TEM sample, followed by the standard sample preparation techniques [11]. Finally, the sample was examined by a Topcon EM-OO2B operated at a 200kV acceleration voltage with the use of the <$\bar{2}$110> zone axis.

Table I. Growth Conditions for the AlN films

Temperature	1050 °C
Al evaporation temperature	1260 °C
Nitrogen flow rate	3.5 sccm
Microwave power	100 W
Growth rate	~17 Å/min

C. Results and Discussion

Figure 1 (a) and (b) shows the initial stage of a deposited AlN film on both on-axis and vicinal 6H-SiC (0001) substrates, respectively. The films show epitaxial 2H (wurtzite) structure which has an ABAB stacking sequence in the <1000> direction, referring to 'ABC' notation. The thickness of the AlN film is ~15Å. Very smooth surface morphological feature and uniformity in thickness can be seen in the AlN film grown on the on-axis substrate (Fig. 1 (a)), indicating a two-dimensional growth mode in this thickness range. In contrast, slightly rougher surface feature can be observed in the AlN film grown on the vicinal surface. Surface roughness is strongly related to the presence of steps in the vicinal surface as indicated by the arrows. Steps may play a role to confine adatoms to create an island within the terrace sites due to step site barriers caused from the strained field of AlN films. This will be discussed later with the use of the structural model at the interface. Higher magnification images of each film, shown in Fig. 2 (a) and (b) can clearly describe the detail of the structures. In Fig. (a), an atomically smooth AlN film surface and an abrupt AlN/SiC interface are seen in the film of the on-axis substrate. The AlN film consists of 5-6 'bi-atomic' monolayers (one 'bi-atomic' layer includes Al (Si) and N (C) layers). On the other hand, island-like surface feature can be observed in the film of the vicinal substrate (Fig. (b)). An island forms on a terrace site which is separated by the steps at each end (see arrows for steps). The film thickness varies from 3-4 to 7-8 monolayers. Coalescent regions of each island have a disordered atomic configuration and form 'valleys' due to misalignment of each island.

In Fig. 3, a model of the AlN/SiC interface including one bi-monolayer step, indicates an anti-phase domain boundary (APB) at the step site. AlN nuclei having ABAB stacking sequence on both of the terrace sites fail to align at the step site because of the difference in the level of 6H-SiC stacking. An 'A' layer of 2H-AlN crystal is rotated 60° from a 'B' layer in the [1000] direction. This model was established on the basis of an assumption: the first AlN layer

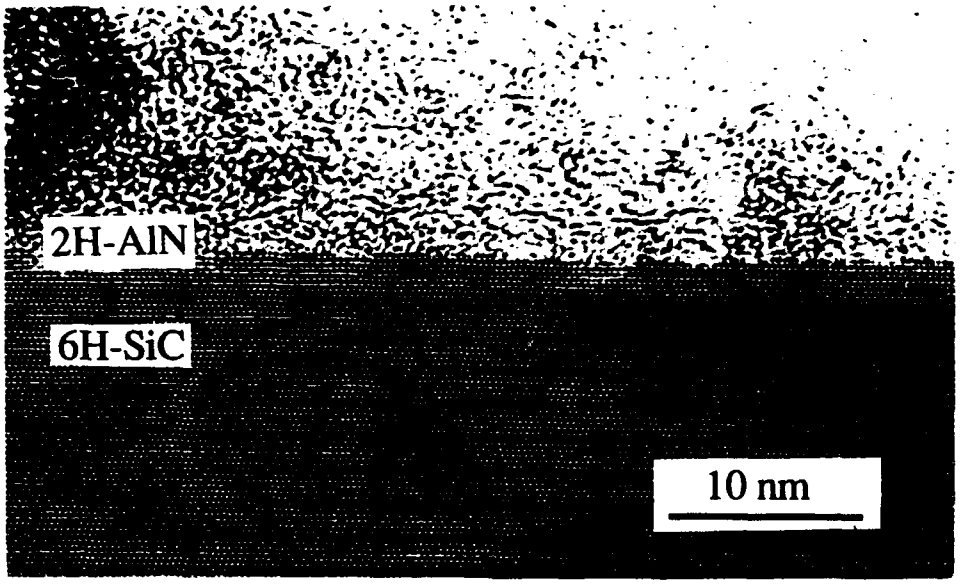

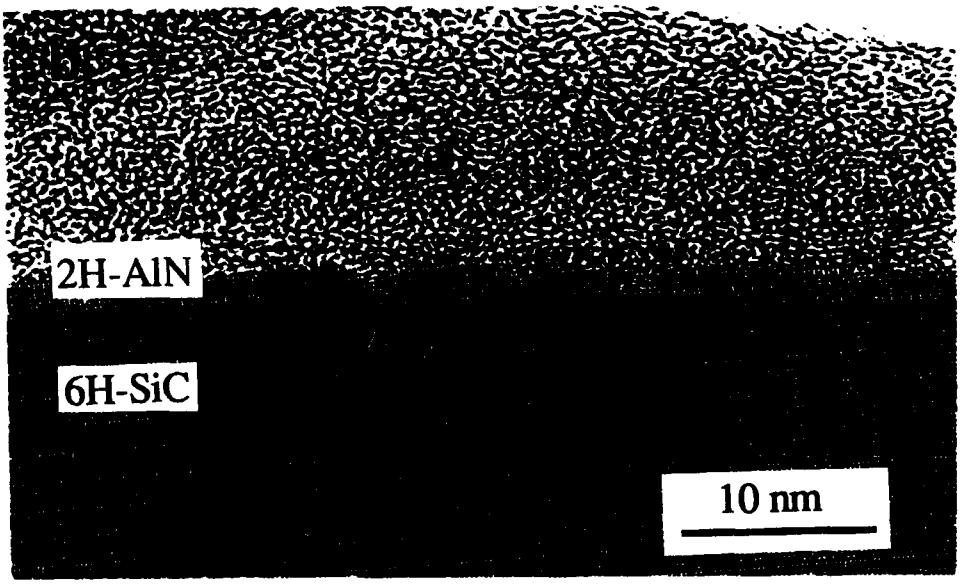

Figure 1. Cross-sectional TEM images of AlN films grown on (a) on-axis substrate and (b) vicinal substrate. The arrows shown in (b) indicate the step positions.

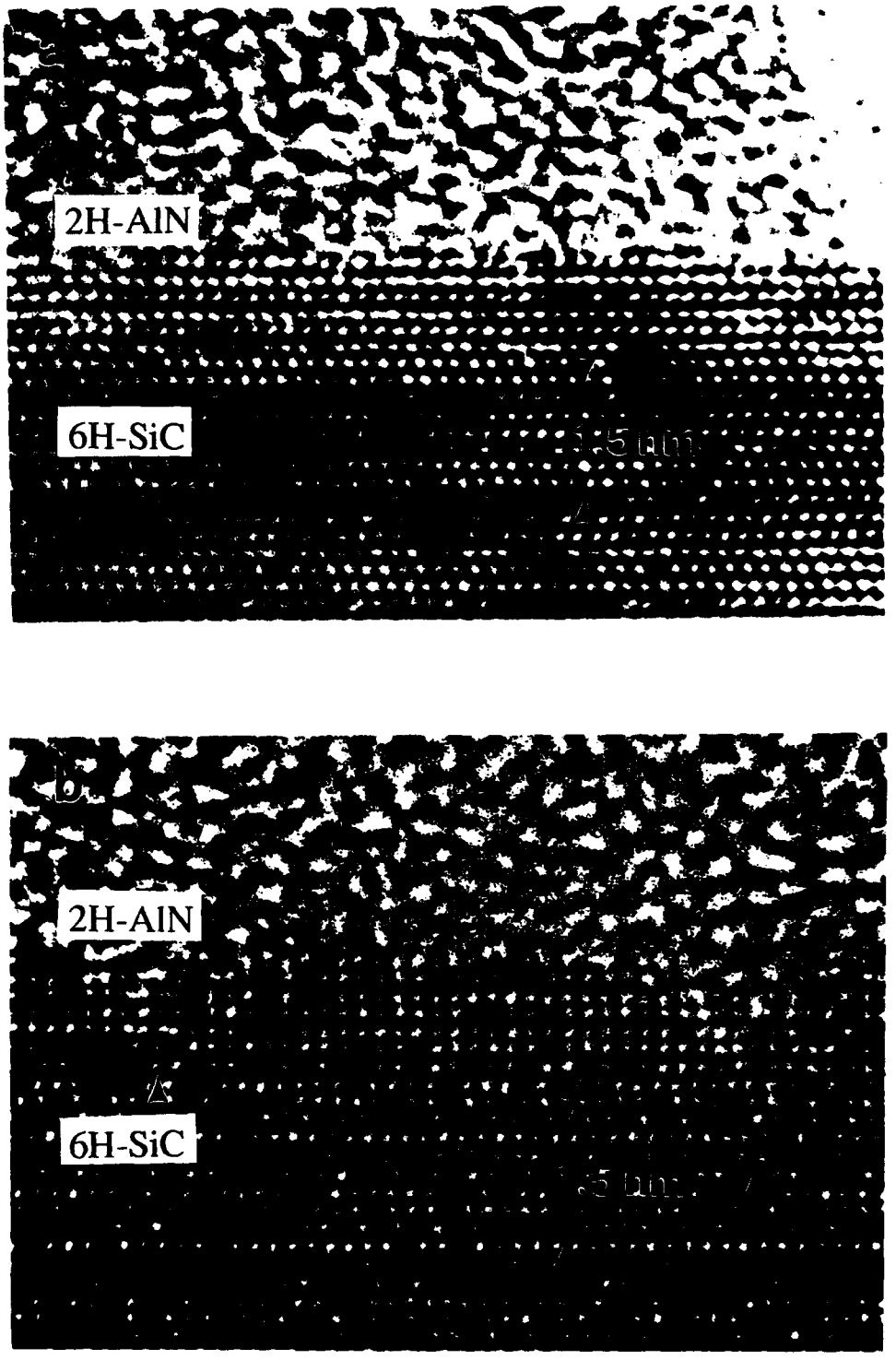

Figure 2. High resolution TEM images of AlN films and AlN/SiC interfaces of (a) on-axis substrate and (b) vicinal substrate. The arrows shown in (b) indicate the step positions.

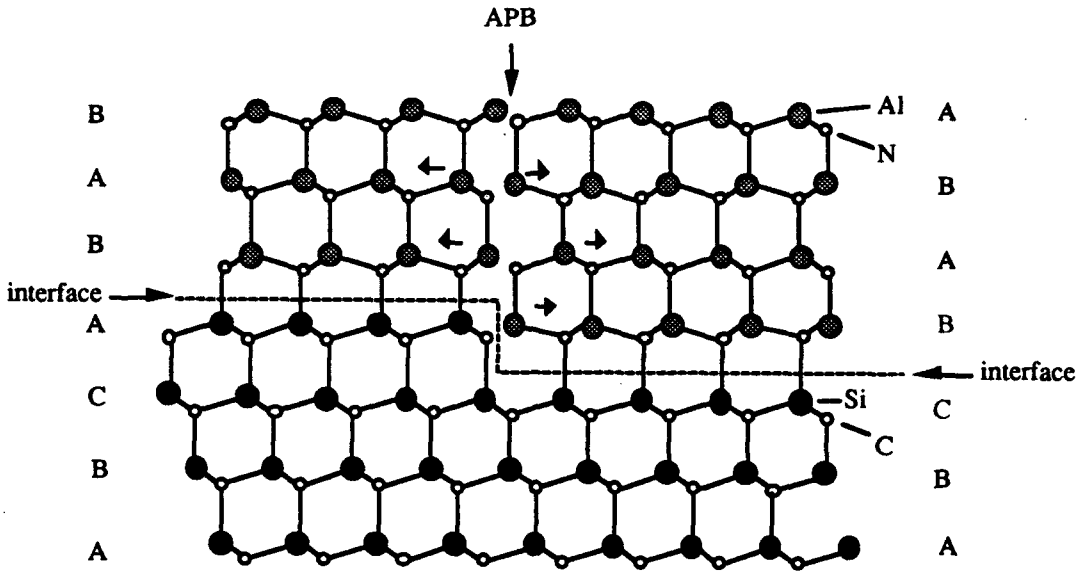

Figure 3. Model of the APB of the AlN/SiC interface. The short arrows indicate the direction of lattice distortion.

energetically prefers to occupy the wurtzite position on the SiC surface, i.e. Al atoms sit on the positions above the C atoms to bond with N atoms. Careful observation of the AlN/SiC interface also suggested the plausibility of this assumption. However, a detailed structural study by quantum mechanical calculations such as shown in the system of Si-$NiSi_2$ and Si-$CoSi_2$ [12] should be made to ascertain this assumption. As indicated by the arrows in Fig. 3, the lattice can be elastically relaxed. Adatoms may feel the strained potential at a step site so that they are hindered to migrate across the surface. Therefore, there is thickness variation which introduces an island formation on the terrace site. Nuclei on the different terrace sites fail to align with the neighboring nuclei (island) due to their anti-phase characteristics. Further study of the step configuration, however, indicates that nuclei formed on different levels of terraces can sometimes align with each other without any strain because of the step geometry of the 6H-SiC substrate [13]. It is clear that an idealistic on-axis SiC surface which includes no steps can provide nearly perfect AlN film growth at the initial stage of growth. A critical thickness for the Stranski-Krastanov growth mode, which might be applied in this AlN/SiC system, will be studied in the series of this research.

D. Conclusion

In summary, the initial stage of 2H-AlN film growth on both on-axis and vicinal 6H-SiC (0001) substrates was investigated by cross-sectional HRTEM. Comparison of very thin films (~15Å) grown on two different surfaces (on-axis and vicinal) shows different surface morphologies and interface micro-structures. A very smooth and defect free AlN film was formed on the on-axis substrate, indicative of a two-dimensional growth mode at this

thickness range. On the other hand, rough and defective features were observed in the AlN film on the vicinal substrate. The high resolution images and the structural model at the interface indicates the presence of APBs due to the nature of steps residing in the 6H-SiC substrate. Finally, it has been suggested that AlN film quality should be improved with the use of an on-axis substrate.

E. Future Plans

The investigation on AlN film growth on 6H-SiC substrates will be continued in terms of suppression of defects and growth mechanisms. The further growth of AlN films will be discussed. The results obtained in this study will be applied for the growth of other systems such as GaN/AlN/SiC and SiC/AlN/SiC. Thus, a similar investigation should be made for SiC growth on AlN surfaces to complete pseudomorphic heterostructural studies.

F. References

1. W. M. Yim, E. J. Stofko, P. I. Pankove, M. Ettenberg, and S. L. Gilbert, J. Appl. Phys. **44**, 292 (1973).
2. M. G. Norton, B. C. H. Steele, and C. A. Leach, Science Ceram. **14**, 545 (1988).
3. G. A. Slack, J. Phys. Chem. Solids **34**, 321 (1973).
4. Z. Sitar, M. J. Paisley, B. Yan, J. Ruan, W. J. Choyke, and R. F. Davis, J. Vac. Sci. Thechnol. **B8**, 316 (1990).
5. L. B. Rowland, R. S. Kern, S. Tanaka, and R. F. Davis, Appl. Phys. Lett. **62**, 3333 (1993).
6. J. H. Edgar, J. Mater. Res. **7**, 235 (1992).
7. S. Strite and H. Morkoc, J. Vac. Sci. Thechnol. **B10**, 1237 (1992).
8. H. Amano, M. Kito, K. Hiramatsu, and I. Akasaki, Jpn. J. Appl. Phys. **28**, L2112 (1989).
9. Cree Research Inc., Durham , NC.
10. L. B. Rowland, R. S. Kern, S. Tanaka, and R. F. Davis, J. Mater. Res. **8**, 2310 (1993).
11. C. H. Carter, Jr., R. F. Davis, and S. R. Nutt, J. Mater. Res. **1**, 811 (1986).
12. D. R. Hamann, Phys. Rev. Lett. **60**, 313 (1988).
13. S. Tanaka, R. S. Kern, and R. F. Davis, paper in progress.

III. Growth of AlN-SiC Pseudomorphic Heterostructures and $(AlN)_x(SiC)_{1-x}$ Solid Solutions by Plasma-assisted, Gas-source Molecular Beam Epitaxy

A. Introduction

A marked increase in the interest in wide band gap semiconductor materials for use in high-temperature, -power, -frequency and -speed microelectronic devices resistant to radiation and short-wavelength optoelectronic devices has recently been demonstrated on a global scale. Two candidate materials that have generated much of this interest are SiC and AlN. Silicon carbide, the only binary compound in the Si-C system, forms in many different polytypes; the most common being the only cubic polytype, β- or 3C-SiC, and one of the hexagonal polytypes, 6H-SiC. Since the band gap for SiC (3.0 eV for 6H and 2.3 eV for 3C) is indirect, it cannot be used alone for optoelectronic applications. For this reason, AlN, with its direct band gap of 6.28 eV, is of particular interest for use with SiC. Two methods of simultaneously exploiting the favorable characteristics of these materials include the thin film deposition of both pseudomorphic heterostructure and alloys.

Pseudomorphic heterostructures of dissimilar semiconductor materials are the basis for quantum well and laser devices. The physical properties (e.g., lattice parameter, crystal structure, melting point and thermal expansion) as well as the optical and electronic properties (e.g., band gap and index of refraction) of SiC and AlN indicate that stable superlattice structures of these materials having the desired properties are feasible. Theoretical calculations regarding electronic structure and bonding at AlN/SiC interfaces [1] and critical layer thickness prior to misfit dislocation formation at interfaces in cubic AlN and SiC have been reported [2]. Rowland *et. al* [3] and Kern *et. al* [4] have described the growth of 3C-SiC/2H-AlN pseudomorphic layers on α(6H)-SiC(0001) substrates by plasma-assisted, gas-source molecular beam epitaxy (PAGSMBE) using solid Al evaporated from a standard effusion cell and the gases of Si_2H_6, C_2H_4 and N_2. The SiC layers contained a high density of stacking faults and microtwins caused primarily by interfacial stresses and the low stacking fault energy intrinsic to β-SiC.

Solid solutions of AlN and SiC have been achieved by two primary processing routes: reactive sintering of mixtures of powders of a variety of sources and thin film deposition from the vapor phase. Matignon [5] first reported the synthesis of a $(AlN)_x(SiC)_{1-x}$ material. Several researchers [6-13] have reported 2H solid solutions as well as mixtures of 6H, 4H, and 2H materials and the existence of a miscibility gap as a result of hot pressing and annealing studies with a variety of heat treatment schedules. The tentative phase diagram proposed by Zangvil and Ruh [10] shows a flat miscibility gap at ≈1900°C between ≈20 and 80 wt% AlN. Above this temperature, a 2H solid solution was reported from ≥20 wt% AlN. For ≤20 wt% AlN,

solutions and two phase mixtures of 6H, 4H, and 2H were observed. Thin film solid solutions have been produced in the Soviet Union [14] via sublimation of a sintered SiC/AlN compact at ≥2100°C and in the United States using low pressure (10–76 Torr) metalorganic chemical vapor deposition (MOCVD) [15] between 1200-1250°C using SiH_4, C_3H_8, NH_3, and $Al(CH_3)_3$ carried in H_2 on α(6H)-SiC(0001) and Si(100) and by PAGSMBE [4, 16] at 1050–1300°C using the sources noted previously [3].

B. Experimental Procedure

In the present research, a specially designed and previously described [17] PAGSMBE system was employed to deposit all AlN-SiC thin films on the Si faces of α(6H)-SiC(0001) substrates. Both on-axis and off-axis (oriented 3.5±0.5° off (0001) toward [11$\bar{2}$0]) SiC substrates were used. The substrates were cleaned chemically before growth in a 10% HF solution for 5 minutes, and loaded immediately into the UHV growth chamber. Sources of Si and C were disilane (Si_2H_6, 99.99% purity) and ethylene (C_2H_4, 99.99% purity), respectively. Aluminum (99.9999% purity) was evaporated from a standard MBE effusion cell operated in all cases at 1260°C. A compact electron cyclotron resonance (ECR) plasma source supplied by ASTeX, Inc., operating at 100 W forward power, was used to decompose N_2 (99.9995% purity). Typical gas flow rates employed for heterostructure growth were 0.1–2.0 sccm Si_2H_6, 0.1–2.0 sccm C_2H_4 (Si/C ratio was kept at 1/1) and 3.5 sccm N_2. Individual layers of SiC and AlN were grown for variable times ranging from 30 seconds to 5 hours. All AlN layers were grown at 1050°C; SiC layers, 1050–1200°C. For solid solution growth, typical flow rates were 0.1–0.5 sccm Si_2H_6 and 0.3–1.5 sccm C_2H_4 (Si/C ratios were kept at 1/3 due to the difficulty previously observed in incorporating C). The N_2 (1.0 sccm) was diluted with 2.5 sccm ultra-high purity Ar (99.999% purity) to obtain sufficient electron-atom collisions to sustain a plasma. All solid solution films were grown at 1200°C on vicinal 6H-SiC(0001) for 2 hours.

Reflection high-energy electron diffraction (RHEED), operating at 10 kV, was used to determine the crystalline quality of the surface of the resulting films. The chemical composition as a function of film thickness was determined using scanning Auger electron spectroscopy (AES). High-resolution transmission electron microscopy (HRTEM) operating at 200 kV was employed to observe the microstructure of the film as well as the film/substrate interfacial region.

C. Results

Multilayer Growth. Figure 1 shows a HRTEM micrograph of a 3C-SiC/2H-AlN/6H-SiC structure grown on vicinal α(6H)-SiC(0001) at 1050°C. The AlN layer was grown for 1 minute using 3.5 sccm N_2 and Al evaporated at 1260°C. The SiC layer was grown for

60 minutes using 0.3 sccm Si_2H_6 and 0.3 sccm C_2H_4. Each layer has an abrupt interface and the atom columns are continuous indicating the structure to be epitaxial and pseudomorphic; however, a significant amount of strain is present in the AlN layer and the 3C-SiC layer shows several <111> stacking faults.

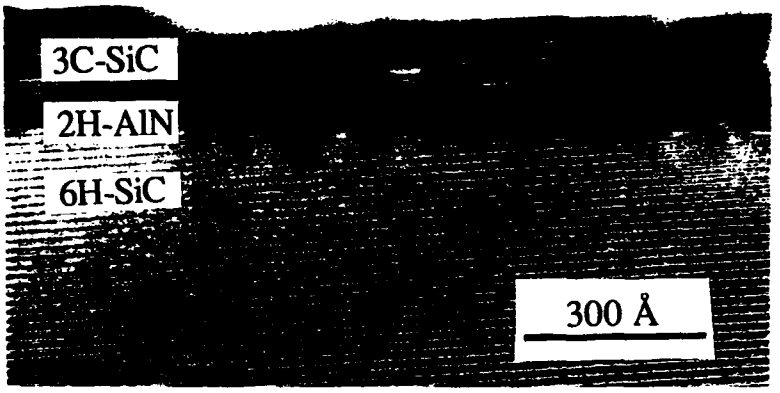

Figure 1. HRTEM micrograph of a 3C-SiC/2H-AlN bilayer grown on vicinal 6H-SiC(0001). Notice the strain present in the AlN layer, seen as lattice fringe distortion, and the <111> stacking faults in the 3C-SiC layer.

Figure 2 shows a HRTEM micrograph of the same structure grown on on-axis 6H-SiC(0001). The layers were grown under identical conditions to those in Fig. 1. The layers here are also epitaxial and pseudomorphic, but the strain and defect density appear to be significantly reduced.

Solid Solution Growth. Solid solution growth in the high-AlN (≥60%) has resulted in polycrystalline films. The highest AlN incorporation achieved was about 80% AlN. The growth conditions used were 0.1 sccm Si_2H_6, 0.3 sccm C_2H_4, 1 sccm N_2 (diluted with 2.5 sccm Ar) and Al (effusion cell at 1260°C) on vicinal 6H-SiC(0001) at 1200°C for 2 hours. Figure 3 shows an AES depth profile of this film.

D. Discussion

In both Figs. 1 and 2, the interfaces are abrupt and uniform and the layers are identically oriented with continuous atom columns indicating that the layers are epitaxial and pseudomorphic. In both cases, the AlN layer is about 15 Å and the SiC layer is about 200 Å thick. However, there is a definite difference in the material quality of the two structures. The structure grown on on-axis 6H-SiC(0001) is far superior in terms of defect density. The exact

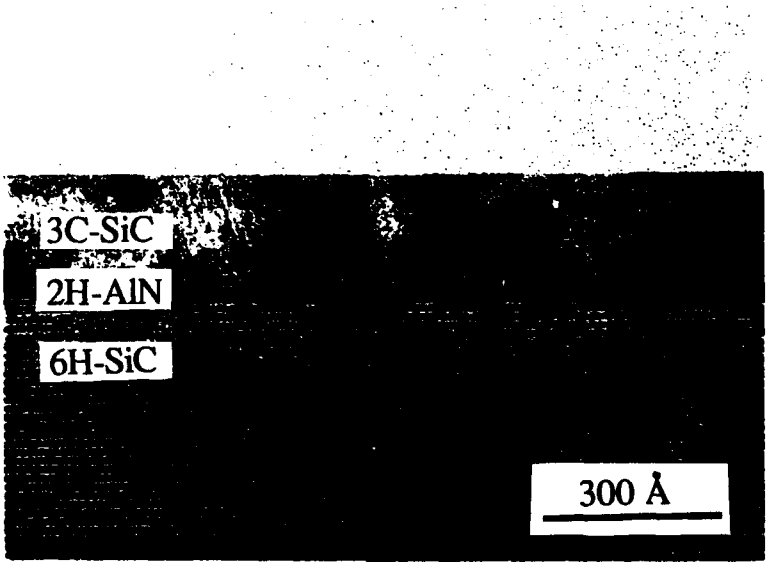

Figure 2. HRTEM image of a 3C-SiC/2H-AlN bilayer grown on on-axis 6H-SiC(0001). Compare the smooth interfaces, reduced strain and low defect density with the image shown in Fig. 1.

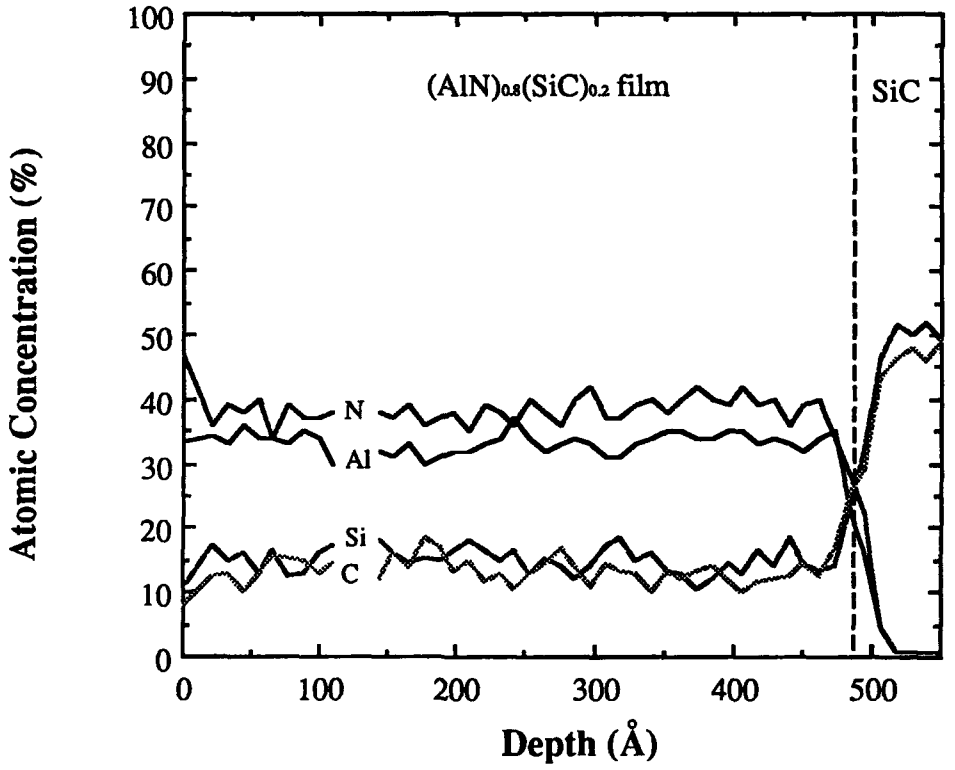

Figure 3. AES depth profile of a polycrystalline $(AlN)_{0.8}(SiC)_{0.2}$ thin film grown on vicinal 6H-SiC(0001).

reasons behind this improvement are not yet understood, but it may present a better means for 3C-SiC growth for use in multilayer heterostructures as well as SIC semiconductor-on-insulator device development.

Previous growth using this system has resulted in low-AlN solid solutions [4, 16]; however, AlN-rich solid solutions have proven to be very difficult to fabricate. The reason for this is not well understood but is thought to be the result of two factors: 1) the relative instability of AlN at high temperatures and low pressures and 2) the strong bonding that occurs between Si and N which may exclude C from incorporating in low-SiC alloys. Figure 3 shows that the constituent can be incorporated at approximately the correct levels, but monocrystalline films have not yet been achieved.

E. Conclusions

Monocrystalline pseudomorphic heterostructures of AlN and SiC have been grown by PAGSMBE on on-axis and vicinal α(6H)-SiC(0001) substrates. The superlattice materials were pseudomorphic and possessed abrupt interfaces regardless of substrate orientation; however, on-axis substrates resulted in far superior structures. High-AlN solid solutions have been achieved, but, to date, these films are polycrystalline.

F. Future Plans and Goals

Further study on the use of on-axis substrates for optimizing growth of β-SiC on AlN to reduce stacking fault densities and improve crystalline quality is currently underway. Attempts to dope the SiC and AlN layers are also underway. Continued work on AlN-rich solid solutions as well as a range of solid solution compositions for use in an annealing study is also planned.

G. References

1. W. R. L. Lambrecht and B. Segall B, Phys. Rev. B **43**, 7070 (1991).
2. M. E. Sherwin and T. J. Drummond, J. Appl. Phys. **69**, 8423 (1991).
3. L. B. Rowland, R. S. Kern, S. Tanaka and R. F. Davis, Appl. Phys. Lett. **62**, 3333 (1993).
4. R. S. Kern, S. Tanaka, and R. F. Davis, to be published in *Proceedings of the International Conference on Silicon Carbide and Related Materials.*
5. C. Matignon, Compt. Rend. hu. L'Acad. Sci. **178**, 1615 (1924).
6. W. Rafaniello, K. Cho and A. V. Vikar, J. Mat. Sc. **16**, 3479 (1981).
7. W. Rafaniello, M. R. Plinchta and A. V. Vikar, J. Am. Ceram. Soc. **66**, 272 (1983).
8. R. Ruh and A. Zangvil, J. Am. Ceram. Soc. **65**, 260 (1982).
9. A. Zangvil and R. Ruh, Mat. Sc. Eng. **71**, 159 (1985).
10. A. Zangvil and R. Ruh, J. Am. Ceram. Soc. **71**, 884 (1988).
11. A. Zangvil and R. Ruh in *Silicon Carbide '87*, American Ceramic Society, Westerville, OH, 1989, pp. 63-82.
12. S. Kuo and A. V. Vikar, J. Am. Ceram. Soc. **73**, 2460 (1990).
13. C. L. Czkaj, M. L. J. Hackney, W. J. Hurley, Jr., L. V. Interrante, G. A. Sigel, P. J. Schields and G. A. Slack, J. Am. Ceram. Soc. **73**, 352 (1990).

14. Sh A. Nurmagomedov, A. N. Pitkin, V. N. Razbegaev, G. K.Safaraliev, Yu M. Tairov and V. F. Tsvetkov, Sov. Phys. Semicond. **23**, 100 (1989).
15. I. Jenkins, K. G. Irvine, M. G. Spencer, V. Dmitriev and N. Chen, J. Cryst. Growth **128**, 375 (1993).
16. R. S. Kern, L. B. Rowland, S. Tanaka and R. F. Davis, J. Mater. Res. **8**, 1477 (1993).
17. L. B. Rowland, R. S. Kern, S. Tanaka, and R. F. Davis, in *Proceedings of the Fourth International Conference on Amorphous and Crystalline Silicon Carbide*, edited by C. Y. Yang, M. M. Rahman, and G. L. Harris (Springer-Verlag, Berlin, 1992), p. 84-89.

IV. Determination of the Diffusivity of Si, C, Al and N at the Interface of the SiC-AlN Diffusion Couple

A. Introduction

Silicon carbide has long been of interest because of its superior structural, thermal and electrical properties. High temperature and/or erosion- and corrosion-resistant wear parts, as well as optoelectronic and microelectronic semiconductor devices, are representative applications. Control of the physical and chemical properties of SiC via microstructural changes achieved by using different processing routes has been extensively studied for many years. The microstructural variables most frequently changed include the amount and the morphology of the various polytypes in the processed material, intentionally-introduced second and additional phases and additions of sintering aids which may or may not form a grain boundary phase. The processing temperature, impurity content, and sintering (or annealing) atmosphere affect the resultant microstructure. However, the primary material remains SiC. Another approach to property engineering involves the alloying of SiC with other ceramic compounds to alter, e. g., the band gap. This approach has also been of interest for several years.

One compound which has been reportedly alloyed with α(6H)-SiC (a_o = 3.08Å) is AlN (a_o = 3.11Å) due to the similarities in the atomic and covalent radii and the crystal structures. Diverse processing routes have been employed to achieve partial or complete solid solutions from these two compounds including reactive sintering or hot pressing of powder mixtures and thin film deposition from the vapor phase [1–12]. There exists, however, a difference in opinion among investigators regarding the occurrence and the extent of solid solutions in the SiC-AlN system at temperatures <2100°C. As such, a research program has been initiated to determine the rates and extent of chemical interdiffusion between deposited monocrystalline AlN (0001) films and α(6H)-SiC (0001) substrates. The progress to date is described in the following sections.

B. Experimental Procedures

Sample Preparation. Samples were prepared in a modified Perkin-Elmer 430 molecular beam epitaxy (MBE) system. Aluminum (99.999%) was evaporated from a standard effusion cell. Activated nitrogen was achieved using an MBE compatible, electron cyclotron resonance plasma source. Single crystal AlN with very few planar defects was epitaxially deposited on vicinal α(6H)-SiC [0001] wafers manufactured by Cree Research, Inc. and cut off axis 3°–4° toward [11$\bar{2}$0]. Growth conditions for the films are presented in Table I.

Table I. Growth Conditions for the 2H AlN films on α(6H)-SiC(0001) substrates

Nitrogen pressure	2×10^{-4} Torr
Nitrogen flow rate	4–5 sccm
ECR microwave power	50 W
Substrate temperature	650°C
Growth rate	≈ 0.1μm/hr
Total growth time	7–8 hrs.

Transmission electron microscopy (TEM) (Hitachi H-800) photos have been taken of the 2H-AlN (wurtzite) film on the α(6H)-SiC substrate before annealing and show a smooth and abrupt interface. Several different precautions were taken in order to prevent contamination of the samples and to minimize the loss of the principal volatile components of aluminum and nitrogen. The samples were placed in a high density pyrolitic graphite crucible shown schematically in Fig. 1. The inside of the crucible was previously coated with SiC by heating

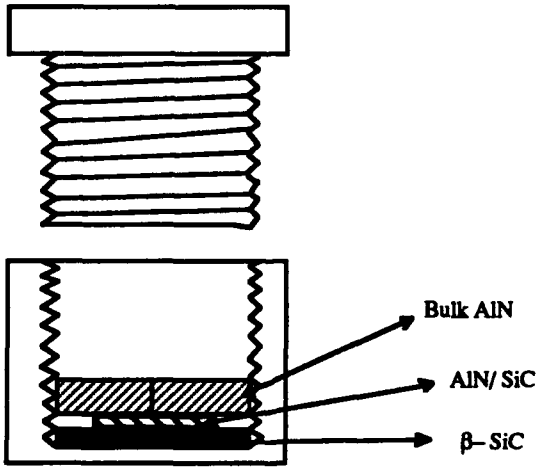

Figure 1. Schematic of a high density pyrolitic graphite crucible.

a mixture of Si and β-SiC inside the holder to 2000°C. The diffusion samples were placed inside this holder with the α(6H)-SiC(0001) face against the SiC coating. Bulk AlN squares cut from a larger piece of Y_2O_3-free AlN previously hot-pressed to essentially theoretical density at Dow Chemical Corporation were then placed on top of each deposited AlN film. The holder was closed using a threaded lid and loaded into the furnace. The chamber was evacuated

(2×10^{-6} torr) to prevent contamination during diffusion. N_2 gas (99.9995%), purified by a gettering furnace containing heated Cu chips (Centorr Furnace model 2B-2O) was then introduced into the chamber at a rate of 500 sccm. The chamber pressure was increased to one atmosphere. A flowing N_2 environment was maintained throughout each diffusion anneal. Diffusion temperatures were reached in ≈40 min., maintained at temperature (±3°C) and cooled rapidly to at least 200°C below the anneal temperature. The N_2 gas, bulk AlN, and SiC-coated crucible were not components in the diffusion process. This was checked using a SiC-AlN standard which had not been annealed. The AlN and the SiC intensities in the standard were the same as the AlN and SiC intensities outside the diffused region. The samples were annealed within the temperature range of 1850°C–1940°C for a period of 25 and 50 hours. A complete listing of temperatures and times are given in Table II.

Table II. Annealing conditions used to date for the AlN/SiC diffusion couples

Temperature (°C)	Time (hrs)
1825	75
1825	100
1850	25
1850	50
1875	50
1875	75
1900	25
1900	50
1940	50

C. Results

The chemical distribution of Al, N, Si and C as a function of depth near the AlN/SiC interface region of two samples were analyzed at Oak Ridge National Laboratory using a Perkin-Elmer Model 660 Scanning Auger Microprobe. The instrument has a primary beam size of 100 nA at 10 keV. The area sputtered on each sample was approximately 250×250 μm at a current of 275 nA. The analysis electron beam sampled the central portion (20× 20μm) of the ion beam sputtered crater.

The sample geometry and ion energy result in an interface resolution of approximately 5–15 nm. However due to sample parameters, such as surface roughness and the atomic sharpness at the interface, ion beam energy distribution parameters, and the large sputtered depth, the resolution at the interface was limited to the larger value of approximately 15 nm.

To quantify the sputtering rate, a depth profile was acquired while simultaneously sampling multiplexed Auger peaks at coarse time intervals. A second depth profile was acquired on a different area of the surface. At the first indication of the SiC substrate, the coarse time intervals were reduced. A diamond stylus profilometer was then used to determine the depth of the sputtered crater. A conversion of sputtering time to depth was calculated by assuming the sputter rate was linear. While penetrating the interface, the sputtered depth between measurements was calculated to be 6 nm. This value is near the lower limit of resolution.

Conversion of the Auger peaks to atomic concentrations is not a completely exact process. Sputtering can distort the composition of the surface layer probed by AES, and Auger electrons that reach the analyzer are emitted from the top 0.5 to 10 nm. Furthermore, inherent uncertainties in the compiled sensitivity factors also influence the atomic concentrations deduced from peak to peak signals derived from differentiated Auger energy spectrum.

Sample 1 was subjected to an 1850 °C annealing for 50 hours, as described earlier. Auger SEM images of the sample are shown in Fig. 2. The region was chosen for analysis because it was relatively free of surface debris. In Fig. 3, the plot of atomic concentration versus depth is shown. The initial concentration of Si and C were due to annealing conditions in a SiC-coated graphite crucible. These initial values in no way affected the diffusion at the interface. The apparent deviations from stochiometry are apparently due to the nature of the sensitivity factors

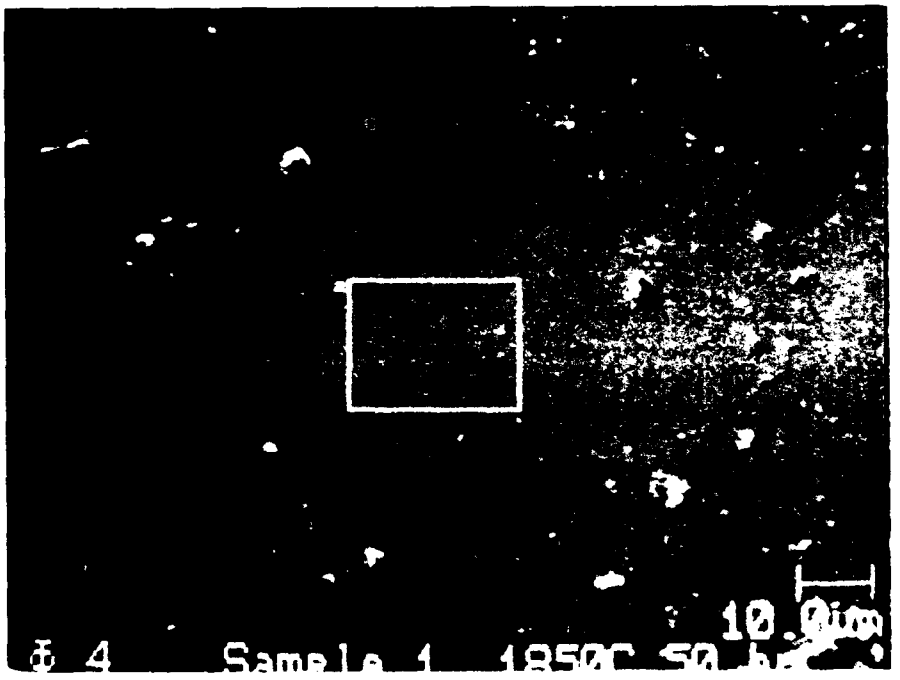

Figure 2. SEM image of sputtering area used for analysis on Sample 1.

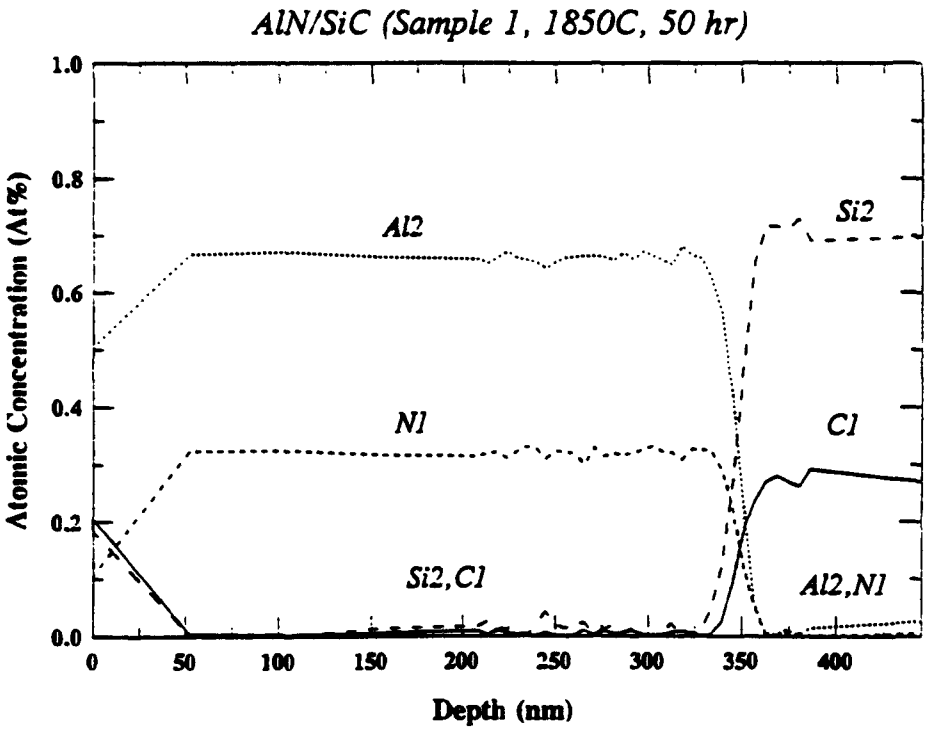

Figure 3. Profile of atomic concentration vs. depth of Sample 1.

in converting the peak height to atomic concentrations. In Fig. 4, an enlarged region of the interface diffusion data is shown. This suggests that an interfacial concentration profile width of no greater than 20 nm. As this distance is approximately the same as the profile resolution at the interface of 15 nm, convincing evidence for chemical interdiffusion has not been observed.

Sample 2 was subjected to a 1900°C annealing for 50 hours. SEM images of the sample are shown in Fig. 5. The region was chosen for analysis because it was relatively free of surface debris. In Fig. 6, the plot of atomic concentration versus depth is shown. The initial concentration of Si and C were again due to annealing conditions in a SiC-coated graphite crucible. In Fig. 7, an enlarged region of the interface diffusion data is shown. This suggests that the interfacial concentration profile width of 30 nm. Although this is greater than profile resolution at the interface and the profiles obtained at 1850°C, it remains sufficiently small such that actual diffusion cannot be confirmed.

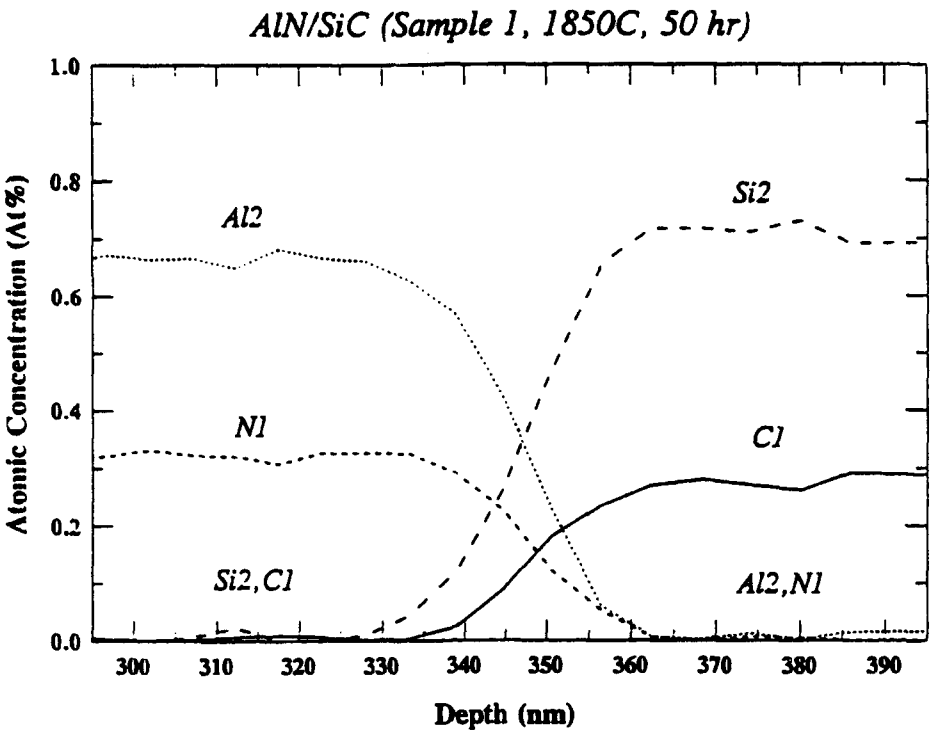

Figure 4. Atomic concentration vs. depth at the interface region. Plot shows interface concentration profile width of approximately 20 nm.

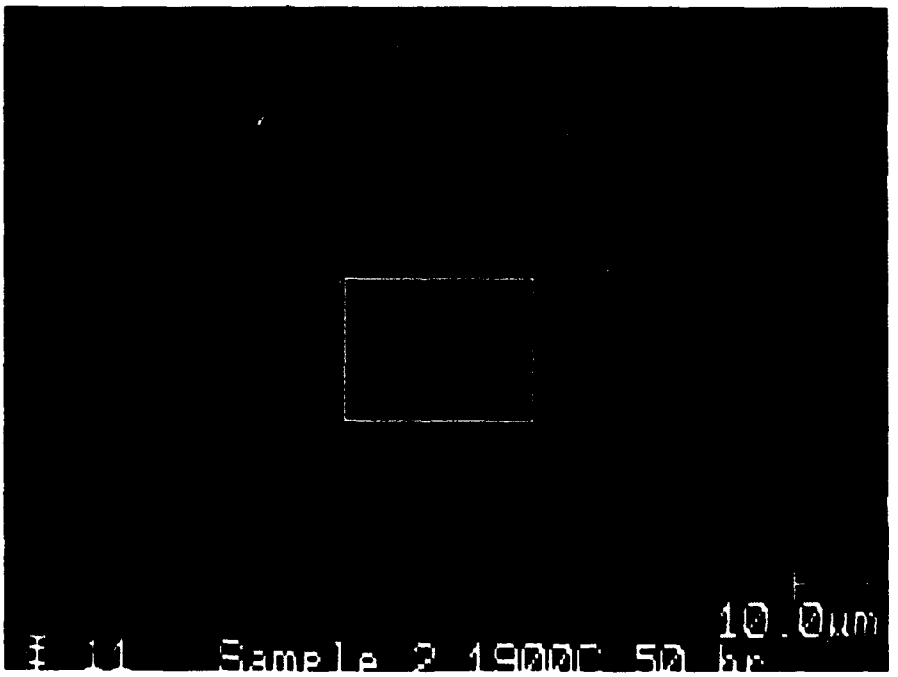

Figure 5. SEM image of sputtering area used for analysis on Sample 2.

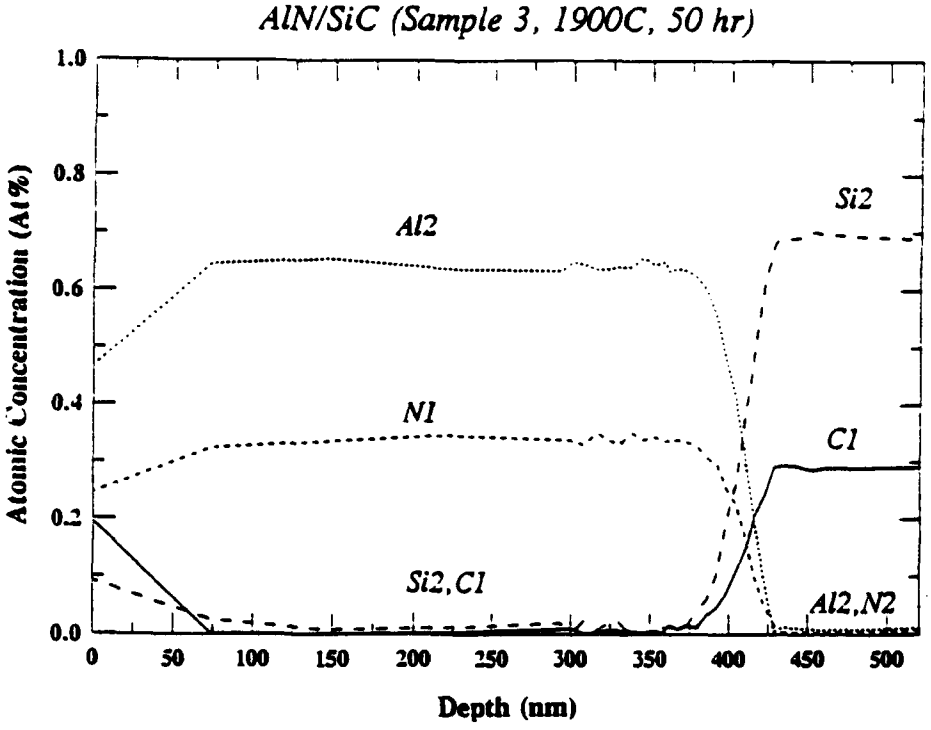

Figure 6. Atomic concentration vs. depth profile of Sample 2.

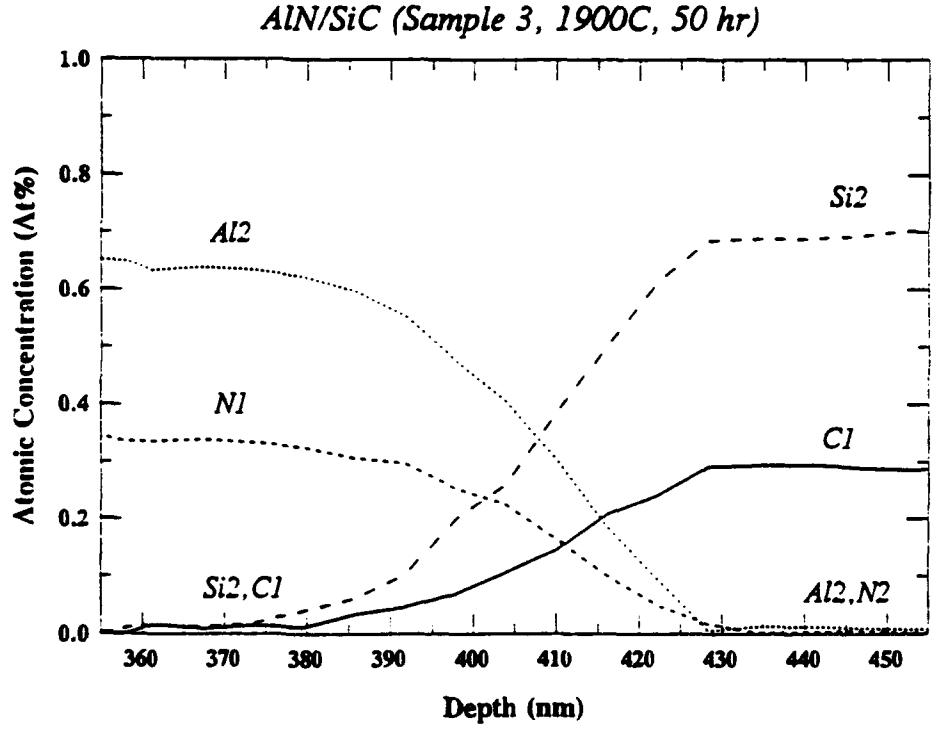

Figure 7. Atomic concentration vs. Depth at interface region. Plot shows interface diffusion width approximately 30 nm.

D. Conclusions

The chemical interdiffusion of Si, C, Al , and N at the interface of two SiC-AlN diffusion couples has been studied. Any diffusion at the interface has been shown to be essentially outside the depth resolution of 15 nm detectabilities of the Auger instrument at the Oak Ridge National Laboratories. This suggests that no interdiffusion occurred in these samples.

E. Future Research Plans and Goals

The diffusion anneals will be completed using the procedure described above. Special care is being taken to ensure a flat AlN surface is achieved after the diffusion experiments and prior to the XPS depth profile studies. Light polishing with diamond paste is being used to produce a flat top surface if it is not present after the diffusion anneals. Additional studies to be conducted in tandem with the diffusion runs include: (1) the fabrication of solid solutions using MBE and the subsequent annealing at high temperatures to determine if either segregation of the AlN and SiC occurs or if the solid solution is maintained and (2) the additional use of parallel electron energy loss spectroscopy via TEM to determine if interdiffusion can be discerned at any temperature.

E. References

1. R. Ruh, A. Zangvil, J. Am. Ceram. Soc. **65** [5], 260 (1982).
2. W. Rafaniello, M. R. Plichta, A. V. Virkar, J. Am. Ceram. Soc. **66** [4], 272 (1983).
3. A. Zangvil, R. Ruh, J. Mat. Sci. and Eng. **71**, 159 (1985).
4. S. Kuo, A. V. Virkar, W. Rafaniello, J. Am. Ceram. Soc. **70** [6], C-125 (1987).
5. W. Rafaniello, K. Cho, A. V. Virkar, J. Mater. Sci. **16** [12], 3479 (1981).
6. I. Jenkins, K. G. Irvine, M. G. Spencer, V. Dmitriev, N. Chen, J. Cry. Gro. **128** 375-378 (1993) .
7. R. S. Kern, L. B. Rowland, S. Tanaka, R. F. Davis, "Solid solutions of AlN and SiC grown by plasma-assisted, gas-source molecular beam epitaxy," J. Mat. Res.
8. Y. Xu, A. Zangvil, M. Landon, F. Thevenot, J. Am. Ceram. Soc. **75** [2], 325-333 (1992).
9. R. Ruh, A. Zangvil, J. Barlowe, Am. Ceram. Soc. Bull., **64** [10], 1368-1373 (1985).
10. L. L. Oden, R. A. McCune, J. Am. Ceram. Soc. **73** [6], 1529-1533 (1990).
11. J. Chen, Q. Tian, A. V. Virkar, J. Am. Ceram. Soc. **75** [4], 809-821 (1992).
12. S. Y. Kuo, Z. C. Jou, A. V. Virkar, W. Rafaniello, J. Mat. Sci. **21**, 3019-3024 (1986).

V. Design and Development of an Ultraviolet Double Heterostructure Light-emitting Diode

A. Introduction

Recent research efforts in the wide-bandgap semiconductor field have concentrated on the development of light-emitting diodes (LEDs) that emit in the blue and ultraviolet wavelengths. The III-V nitrides are most promising candidate materials for the development of highly efficient LEDs that emit in this spectral range because they possess three favorable characteristics: (1) they all have direct transition band structures, (2) their transition band energy levels correspond to the UV and blue spectral range, and (3) they can be mixed to form solid solutions allowing for the tailoring of bandgap energies to specific wavelengths. Within the past several years, significant advances in GaN and AlN growth techniques have been achieved [1-10]. Consequently, high quality epitaxial films that exhibit remarkably improved surface morphologies can now be produced by CVD and MBE methods. Additionally, researchers have successfully doped the III-V nitrides and their alloys creating n-type (Si, Ge) doped films [11-13] and more notably, p-type magnesium doped films [4,9,12]. These recent developments provide all of the material ingredients necessary for the fabrication of efficient blue and UV LEDs.

Some of the earlier LEDs were constructed of simple p-n junctions of GaN. Although the devices did emit light, they lacked the efficiency required for practical applications [13,16]. Further refinements on the device designs were developed to enhance the LED characteristics. By combining growth techniques leading to the construction of a double heterostructure single quantum well and doping the confining layers, the efficiency of the resulting LED could be further optimized by improving the carrier confinement and mobility. Recently, several successful attempts have been reported in the fabrication of double heterostructure (blue, UV) light emitting diodes [12-19]. All of these efforts have used either MOCVD or MOVPE growth techniques. Most designs are GaN based, using $Al_xGa_{1-x}N$ solid solutions for UV emissions, and $In_xGa_{1-x}N$ solid solutions for blue emission. All of the devices fabricated used sapphire substrates and either AlN or GaN buffer layers. A typical double heterostructure design is shown schematically in Fig. 1. In this report, the initial steps of fabricating such a structure by GSMBE are investigated, including attainment of compositional control of the $Al_xGa_{1-x}N$ solid solution and control of the deposition rate to achieve desired confinement layer thicknesses.

B. Experimental Procedure

GaN/AlGaN double heterostructures were grown on (0001) oriented α(6H)-SiC wafers provided by Cree Research, Inc. The films were grown by ECR assisted GSMBE using a commercial Perkin-Elmer 430 system. The Al and Ga fluxes were provided by

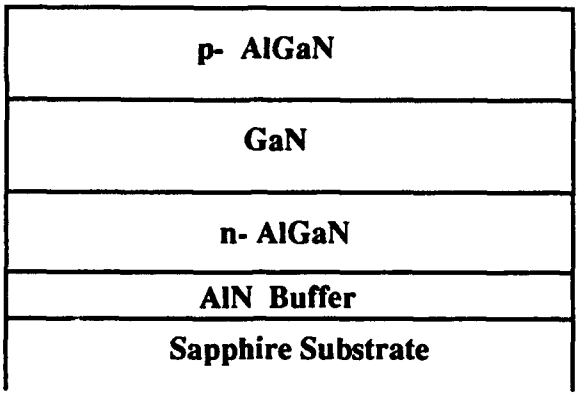

Figure 1. Typical double heterostructure.

standard Knudson effusion cells. The N_2 source gas, ultra-high purity, was excited by an ECR plasma source. The ECR was designed to fit inside a standard effusion cell sleeve (2.25" diameter) [1]. All substrates were cleaned by a standard degreasing and RCA cleaning procedure prior to loading into the system. Additionally, the substrates were degassed at 700°C for 30 minutes prior to transferring to the deposition chamber.

Four double heterostructure samples were grown, each consisting of a GaN active layer between two AlGaN confinement layers. Prior to depositing the first AlGaN confinement layer, an AlN buffer layer was deposited on the SiC surface. Compositional ratios of Al-atoms to the Ga-atoms in the $Al_xGa_{1-x}N$ confinement layers were varied through control of the Ga-cell and Al-cell temperatures. Initial cell and growth temperatures were based on previous research conducted by our group [20]. The multilayered structure was obtained by operating the effusion cell shutters to abruptly start or stop the Al and/or Ga flux.

C. Results and Discussion

The goal in this aspect of research has been directed at attaining compositional control of the $Al_xGa_{1-x}N$ solid solutions in the range of $0.1<x<0.4$, and control of the deposition rates to achieve the desired layer thicknesses. Typical deposition conditions are listed in Table I. Reflection high-energy electron diffraction (RHEED) was used to examine the crystalline quality of the top AlGaN layer. In all four samples, the RHEED pattern indicated good crystalline quality. The chemical composition as a function of film thickness was determined using scanning Auger electron spectroscopy (AES). Results of an AES depth profile performed on sample 4 are shown in Fig. 2. Cross-sectional Scanning Electron Microscopy (SEM) was used to measure the layer thicknesses. The effects of cleaving the samples for SEM analysis and the relatively low concentration of Al in the AlGaN layers limited the ability of distinguishing between the different layers using this analysis. Only in the case of sample 4

Table I. Deposition Conditions for GaN / AlGaN Double Heterostructures

Nitrogen pressure	2×10^{-4} Torr			
Microwave power	50 W			
Substrate Temperature	650°C			
Sample number	1	2	3	4
Target x-value	0.1	0.2	0.3	0.4
Ga cell temperature	985°C	980°C	975°C	970°C
Al cell temperature	1040°C	1060°C	1080°C	1100°C
Ga/Al flux ratio	6.7	4.3	2.1	1.3

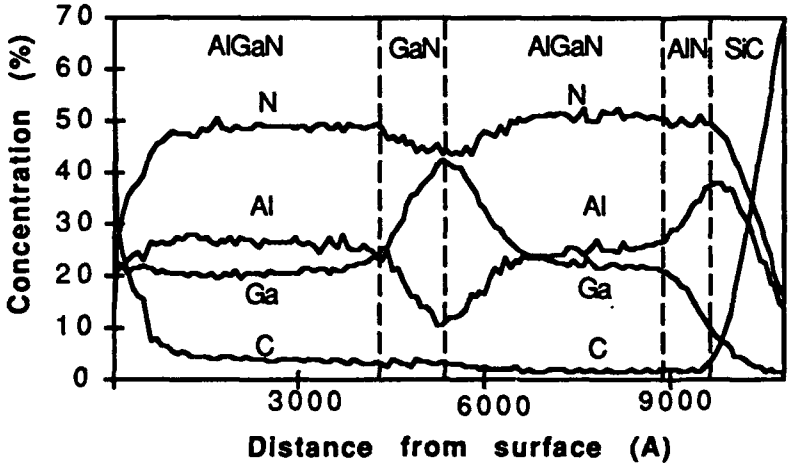

Figure 2. Auger depth profile of AlGaN/GaN/AlGaN double heterostructure.

were we able to successfully employ this technique. The results indicated that using the parameters listed in Table I for sample 4, growth rates of 1350 A/hr, 600 A/hr, and 2300 A/hr for GaN, AlN, and AlGaN respectively were achieved. Analysis of Figure 2 also indicates a solid solution composition of approximately $Al_{0.6}Ga_{0.4}N$. Based on previous results using AES analysis (20), the composition at these growth parameters resulted in a composition of approximately $AL_{0.4}Ga_{0.6}N$. Some of this discrepancy can be accounted for by lack of an appropriate solid solution standard used for calculation of the composition. This limits the

ability to correctly account for the sensitivity factors used in compositional determination. A more accurate method of determining the AlGaN composition needs to be used in order to attain the required control of Al/Ga ratios in the confinement layers necessary for efficient LEDs and ultimately injection laser fabrication.

D. Conclusions

Pseudomorphic double heterostructures of GaN/AlGaN with varying solid solution compositions were grown using ECR assisted GSMBE. Layer growth rate determination using SEM was hindered by film cleavage effects and poor layer contrast due to low Al concentrations in the AlGaN layers. Only in the case where the Al concentration was relatively high (x=0.4) was an accurate determination made using this technique. Results from AES depth profiling indicate the double heterostructure exhibits abrupt interfaces, however use of AES for accurately determining the layer compositional ratios is limited.

E. Future Research Plans and Goals

Improvement on layer thickness determination by cross-sectional SEM will be addressed. The existing double heterostructure cleaved faces will be ground and polished prior to SEM analysis. This should improve the imaging ability by removing the effects that result from cleaving the film. Also, the use of reactive ion etching (RIE) of selected layers will be investigated as a possible aid to enhance the use of SEM analysis as a technique for layer thickness determination.

Additionally, single layers of AlGaN solid solutions will be grown on α(6H)-SiC and the composition will be determined using X-ray diffraction analysis. This should result in a more reliable measurement than that provided by AES analysis.

Once we have acquired the control over the solid solution composition and growth rate of the individual layers needed for device fabrication, we will expand our studies to include doping of the confinement layers, specifically p-type (Mg) and n-type (Ge).

The second stage in the development of the UV LED, once the growth parameters have been determined for achieving the desired composition and growth rate, will be the deposition of the underlying structures for the double heterostructure design. Having selected the AlGaN/GaN system for the basis of the LED, and using GaN as the active layer, the emitted light should exhibit a wavelength in the UV-spectral region (bandgap energy = 3.45ev corresponding to 360 nm). The choice of substrate is α-SiC which will provide for the growth of better quality films than those grown on sapphire [21]. The films will be deposited as shown schematically in Fig. 1. Various growth conditions will be used to control such designs encompassing active layer thickness and AlGaN doping with Mg and Ge. Selection of the active layer thickness will be made considering the effects of strain induced bandgap shifts,

critical thickness of the GaN layer, and composition of the alloy confinement layers [22-24]. After the structures have been grown, the devices will be fabricated using RIE for mesa formation. Optical characterization of the final LED designs will include photo- and cathodoluminescence.

F. References

1. Z. Sitar, M. J. Paisley, D. K. Smith and R. F. Davis, Rev. Sci. Instrum. **61**, 2407 (1990).
2. K. Hirosawa, K. Hiramatsu, N. Sawaki and I. Akasaki, Jpn. J. Appl. Phys. **32**, L1039 (1993).
3. S. Yoshida, S. Misawa and S. Gonda, J. Appl. Phys. **53**, 6844 (1982).
4. C. Wang and R. F. Davis, Appl. Phys. Lett. **63**, 990 (1993).
5. S. Nakamura and T. Mukai, Jpn. J. Appl. Phys. **31**, L1457 (1992).
6. T. Nagatomo, T. Kuboyama, H. Minamino and O. Omoto, Jpn. J. Appl. Phys. **28**, L1334 (1989).
7. M. A. Khan, J. M. Van Hove, J. N. Kuznia and D. T. Olson, Appl. Phys. Lett. **58**, 2408 (1991).
8. N. Yoshimoto, T. Matsuoka, T. Sasaki and A. Katsui, Appl. Phys. Lett. **59**, 2251 (1991).
9. S. Nakamura, M. Senoh and T. Mukai, Jpn. J. Appl. Phys. **30**, L1708 (1991).
10. J. Sumakeris, Z. Sitar, K. S. Ailey-Trent, K. L. More and R. F. Davis, Thin Solid Films **225**, 244 (1993).
12. I. Akasaki, H. Amano, N. Koide, M. Kotaki and K. Manabe, Physica B **185**, 428 (1993).
13. N. Koide, H. Kato, M. Sassa, S. Yamasaki, K. Manabe, M. Hashimoto, H. Amano, K. Hiramatsu and I. Akasaki, J. Crystal Growth **115**, 639 (1991).
14. M. A. Khan, D. T. Olson, J. M. Van Hove and J. N. Kuznia, Appl. Phys. Lett. **58**, 1515 (1991).
15. S. Nakamura, M. Senoh and T. Mukai, Appl. Phys. Lett. **62**, 2390 (1993).
16. B. Goldenberg, J. D. Zook and R. J. Ulmer, Appl. Phys. Lett. **62**, 381 (1993).
17. S. Nakamura, M. Senoh and T. Mukai, Jpn. J. Appl. Phys. **32**, L8 (1993).
18. I. Akasaki, H. Amano, H. Murakami, M. Sassa, H. Kato and K. Manabe, J. Crystal Growth **128**, 379 (1993).
19. H. Amano, N. Watanabe, N. Koide and I. Akasaki, Jpn. J. Appl. Phys. **32**, L1000 (1993).
20 December 1992 Annual Report, Grant #N00014-92-J-1720
21. S. Strife and H. Morkoc, J. Vac. Sci. Technol. B **10**, 1237 (1992).
22. S. Krishnankutty, R. M. Kolbas, M. A. Kahn, J. M. Van Hove and D. T. Olson, J. Electron. Mater. **21**, 609 (1992).
23. M. A. Kahn, R. A. Skogman, J. M. Van Hove, S. Krishnankutty and R. M. Kolbas, Appl. Phys. Lett. **56**, 1257 (1990).
24. S. Krishnankutty, R. M. Kolbas, M. A. Kahn, J. N. Kuznia, J. M. Van Hove and D. T. Olson, J. Electron. Mater. **21**, 437 (1992).

VI. Deposition of Gallium Nitride Via Supersonic Jets

A. Introduction

The nitride family of materials, GaN, AlN and InN as well as their solid solutions offer the possibility of new high-power and high-temperature devices. These materials have direct band gaps of 3.4, 6.28 and 1.95 eV, respectively. They form solid solutions with each other offering a wide range of possible band gaps [1]. GaN has a high electron drift velocity and would be suitable for high-frequency and microwave devices [1,2]. However considerable efforts have been guided toward obtaining p-type or insulating GaN [2,3]. Glaser *et.al.* [4] proposed a model based on native N vacancies to explain the n-type nature of GaN. To minimize the concentration of N vacancies, low temperature growth methods have been pursued. These methods include electron cyclotron resonance (ECR) microwave-plasma assisted molecular beam epitaxy, atomic layer epitaxy , ECR plasma enhanced metal organic vapor phase epitaxy and reactive magnetron sputtering [1,3,5-7]. The use of low temperature processes has also been reported to produce films with improved surface morphology [5]. Newman et.al. proposed that the growth of GaN at low temperatures proceeds as a metastable process. Activated N species are required to overcome the kinetic barrier for GaN formation. The formation of GaN is controlled by the arrival of activated N species to the substrate surface. The decomposition of GaN is hindered by a large kinetic barrier [7]. NH_3 and N_2 are the most common N sources utilized for GaN film growth [1,6,8,9]. NH_3 can be decomposed thermally at substrate temperatures of 600°C to produce NH radicals which adsorb onto the substrate [8]. N_2 is used with the assistance of a plasma source to produce activated N species. This allows GaN to grow at substrate temperatures as low as 450°C [9].

In the present project we propose to use Supersonic Jet Deposition (SJD) to grow GaN at low temperatures (i.e. 300°C). In SJD a diluted mixture of a gas phase Ga precursor and a N precursor are expanded through a small (≈100μm) orifice from a high pressure reservoir (P_o) into a low pressure chamber (P_b). If the ratio (P_o/P_b) is greater than 2 the expanded species will attain an average velocity equal to the speed of sound. This is due to the conversion of the thermal energy or enthalpy of the species in the reservoir into directed kinetic energy. The ultimate velocity V, that the species will attain depends on the reservoir temperature T_o, and the molecular weight of the gas W, by the following equation [10]:

$$V = M\sqrt{\frac{\Omega R T_o}{W}}\left[1+\frac{\Omega-1}{2}\right]^{\frac{-\Omega}{\Omega-1}}$$

where Ω is the ratio of the heat capacities at constant pressure and volume, R is the universal gas constant, and M is the Mach number. M is a measure of the conversion of enthalpy into

kinetic energy [11]. If the carrier gas used to dilute the precursors is lighter than the precursors, during the expansion the heavier species attain the velocity of the lighter species [10]. This occurs because of elastic collisions between the gas molecules during the expansion. The variation of temperatures, carrier gases and precursors allows for the generation of activated species with kinetic energies ranging from 0.1 to 20 eV [10-12]. With SJD it is possible to produce molecular beams with low energy spreads. The energy spread is controlled by the local beam temperature which is related to P_o/P_b via the following equation:

$$\frac{P_b}{P_o} = \left[\frac{T}{T_o}\right]^{\frac{\Omega}{\Omega-1}}$$

where T is the local gas temperature which is a function of distance away from the nozzle. As P_b/P_o decreases, T decreases as shown by the equation above [10]. The lower this local temperature the narrower the local kinetic energy distribution. Supersonic beams with energy spreads in the meV range have been reported for fundamental surface studies [12].

The gases emerging from the free jet can be passed through a skimmer to extract a supersonic molecular beam. During the supersonic expansion a mach disk is formed at a distance dependent on P_o/P_b via the following equation [10]:

$$\frac{X_m}{d} = 0.67\left[\frac{P_o}{P_b}\right]^{\frac{1}{2}}$$

where X_m is the mach disk distance from the nozzle, and d is the nozzle diameter.

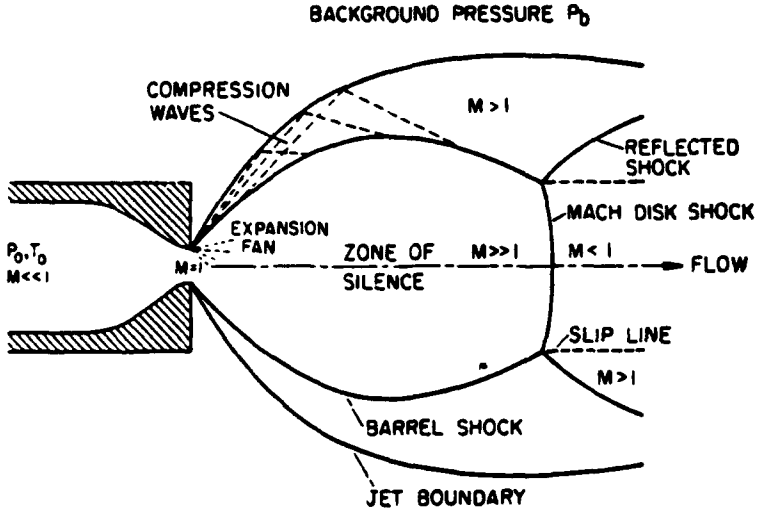

Figure 1. Supersonic Jet expansion diagram.

The mach disk distance is the distance from the orifice where the velocity of the gas molecules goes from supersonic to subsonic due to shock waves around the "zone of silence"

(Fig. 1 - taken from ref. 10, p. 15). The zone of silence is the zone in the expansion where the largest number of collisions between gas molecules occur. The gas attains a supersonic velocity in this area. Outside the zone of silence a shock wave structure is formed. If a skimmer is placed within the mach disk distance, the extracted beam will be in the free molecular flow regime and will travel at supersonic velocities [10,12]. When using the free jet deposition mode it is important however that the sample be within the mach distance.

Ceyer (13) studied the effect of kinetic energy on the dissociative chemisorption of CH_4 on Ni (111) substrates. It was shown that the probability for dissociative chemisorption of CH_4 increased linearly with increase in translational energy of the molecule. This was correlated to the distortion of the C-H bonds upon collision of CH_4 onto the substrate. At high kinetic energies the deformation of the bonds allows the C atom sees the surface and a CH radical adsorbs giving off H atoms. Eres and Sharp [14] showed that Ge deposited on Ge (100) substrates was a result of a chemisorption reaction. They also found that growth of subsequent layers was controlled by the desorption of H from the adsorbed Ge.

Si and Ge have been deposited using supersonic jets. Eres *et al.* deposited Ge on GaAs by pulsed SJD [15]. The pulsed mode of SJD follows the same principles previously explained, but the nozzle is opened for short time intervals and then closed creating pulses of gas. Eres *et al.* used digermane (Ge_2H_6) as a precursor and He as a diluent. They observed very high epitaxial growth rates (0.25 μm/s), two orders of magnitude higher than in CVD at the same temperatures. They also estimated that 75% of the digermane came in contact with the substrate. The film growth efficiency was calculated to be 0.01 [15]. In another study Eres *et al.* showed that the crystallinity of the film could be controlled by SJD to give amorphous films at very high deposition rates [16]. This is in agreement with kinetics as the growth rate of Ge is a function of the arrival rate and decomposition rate of Ge_2H_6 on the GaAs. Under low Ge_2H_6 exposures, the deposited Ge is allowed to diffuse along the surface and form a highly crystalline structure. At high fluxes the arrival rate prevents the atoms from diffusing along the surface to form a crystalline structure and, therefore, an amorphous structure is developed.

Ohmi *et al.* [17] grew homoepitaxial Si films at growth rates of 0.5 μm/min. Films with low defect concentrations and little contamination were obtained at temperatures as low as 600°C . The growth mechanism was found to be dominated by the chemical decomposition on the surface of the substrate. Disilane (Si_2H_6) was used as a precursor. Zhang *et al.* [18] grew GaAs by a pulsed mode SJD. Trimethyll gallium (TMG) was used as the Ga precursor. The substrate was continuously exposed to AsH_4. The epitaxial growth was controlled by adjusting the TMG source pulse width. This provides a means to control the individual submonolayer growth.

The purpose of this study is to grow and characterize GaN films made via SJD using triethyllgallium (TEG) and ammonia (NH_3) as precursors. It is proposed that the surface

decomposition of these precursors will be aided by the translational kinetic energy obtained during the expansion. The translational kinetic energy might also aid the surface diffusivity of the deposited species. This effect of the translational energy will allow for the deposition of crystalline films at low temperatures (200-600°C).

B. Experimental procedure

Figure 2 is a schematic of the SJD unit used to deposit GaN. The unit consists of two chambers which allow for the placing of a skimmer to collimate the free jet and extract a molecular beam. The back chamber (II) is pumped by a 10" diffusion pump backed by a mechanical pump giving a total pumping speed of 3300 l/s. The front chamber (I) is pumped by a 8" diffusion pump backed by a roots blower and a mechanical pump giving a total pumping speed of 6600 l/s. The base pressure of the system is 10^{-6} torr. During deposition in the free jet mode the front chamber pressure is 10^{-4} torr and the back chamber pressure is 10^{-3} torr. If a skimmer is used the front chamber pressure will be 10^{-3} and the back chamber pressure will be 10^{-4} torr. The nozzle is made of a 1.5" steel tube which accommodates pinholes of sizes varying from 10μm to 250μm. The nozzle can be heated using a resistive coil heater. The sample is heated by an infra red (IR) lamp. Before each deposition the system is pumped down to the base pressure. He is the TEG carrier gas and diluent. TEG and NH_3 will be mixed within the nozzle reservoir prior to the expansion.

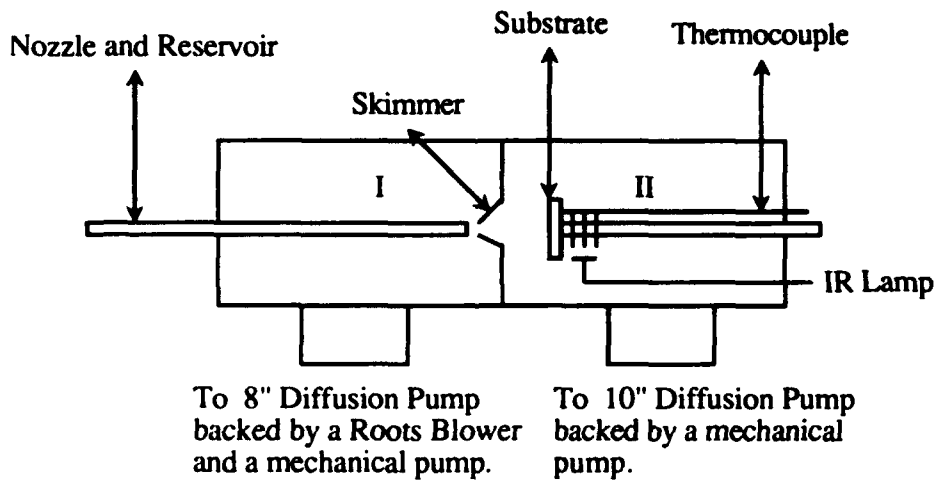

Figure 2. Schematic of SJD GaN deposition unit (supersonic molecular beam mode).

A free jet mode as well as a collimated molecular beam mode will be used to deposit GaN. The growth will be studied as a function of nozzle temperature, beam or jet composition, deposition time, reservoir pressure, nozzle to sample distance, substrate temperature and

deposition mode. The films will be characterized to determine composition, surface morphology, crystallinity, microstructural properties and electrical properties using Auger electron spectroscopy (AES), scanning electron microscopy (SEM), X-ray diffraction (XRD) transmission electron microscopy (TEM) and Hall measurements respectively. The SJD unit was completed and installed recently. Initial testing has begun with detailed experimentation forthcoming.

C. Future Research Plans and Goals

The initial stages of experimentation will focus on depositing Ga and N on the surface of Si (0001) wafers. The temperature and beam composition will be varied to optimize the stoichiometry and crystallinity of the film. Once the deposition on Si is achieved, SiC will be used as a substrate and the growth conditions of the films will be optimized to yield crystalline, stoichiometric, low defect density and uniform surface morphology. Details about the growth mechanism will be also pursued.

D. Bibliography

1. T. Lei, T.D. Moustakas, R.J. Graham, Y. He and S.J. Berkowitz, J. Appl. Phys. **71(10)**, 4933, (1992).
2. M. J. Paisley, Z. Sitar, J. B. Posthill and R. F. Davis, J. Vac. Sci. Technol. **A7(3)**, 1989.
3. Cheng Wang and R.F. Davis, Appl. Phys. Lett. **63(7)**, 990, (1993).
4. E. R. Glaser, T. A. Kennedy, J. A. Freitas Jr., M. Asif Khan, D. T. Olson and J. N. Kuznia, presented at the International Conference on Silicon Carbide and Related Materials (ISCRM), Washington, D.C., 1993.
5. S. Zembutsu, and T. Sasaki, Appl. Phys. Lett. **48(13)**, 870, (1986).
6. J. Sumakeris, Z. Sitar, K. S. Ailey-Trent, K. L. More and R. F. Davis, Thin Solid Films **225**, 244-249, (1993).
7. N. Newman, J. Ross and M. Rubin, Appl. Phys. Lett. **62(11)**,1242, (1993).
8. R. C. Powell, N. E. Lee and J. E. Greene, Appl. Phys. Lett. **60(20)**, 2505, (1992).
9. R. C. Powell, N. E. Lee, Y. W. Kim and J. E. Greene, Appl. Phys. Lett. **73(1)**, 189, (1993).
10. D.Eres, D. H. Lowndess and J. Z. Tischler, J. Vac. Sci. Technol. A **11(5)**, 2463 (1993).
11. D.Eres, D. H. Lowndess, J. Z. Tischler, J. W. Sharp, T. E. Haynes and M. F. Chisholm, J. Appl. Phys. **67(3)**, 1361 (1990).
12. T. Ohmi, M. Morita, T. Kochi, M. Kosugi, H. Kumagai amd M. Itoh, Appl. Phys. Lett. **52(14)**, 1173, 1988.
13. S. Zhang, J. Cui, A. Tanaka, Y. Agoyagi, Appl. Phys. Lett. **64(9)**, 1105, (1994).
14. S. T. Ceyre, J. D. Beckerle, M. B. Lee, S. L. Tamg, Q. Y. Yang and M. A. Hines, J. Vac. Sci. Technol. A **5(4)**, 501 (1987).
15. D.Eres and J.W. Sharp, J. Vac. Sci. Technol. A **11(5)**, 2463 (1993).
16. Giancinto Scoles Ed., Atomic and Molecular Beam Methods **1**, Oxford University Press, New York 1988.
17. R. Campargue, J. Phys. Chem. **88**, 4466-4474 (1984).
18. H. Haberland, U. Buck and M. Tolle, Rev. Sci. Instrum. **56(9)**, 1712 (1985).

VII. Distribution List

Mr. Max Yoder Office of Naval Research Electronics Division, Code: 1114SS 800 N. Quincy Street Arlington, VA 22217-5000	3
Administrative Contracting Officer Office Of Naval Research Resident Representative The Ohio State University Research Center 1960 Kenny Road Columbus, OH 43210-1063	1
Director, Naval Research Laboratory ATTN: Code 2627 Washington, DC 20375	1
Defense Technical Information Center Bldg. 5, Cameron Station Alexandria, VA 22314	12